Synthesis, structure and antifungal properties of Co(II)–sulfathiazolate complexes

Sebastián Bellú [a], Estela Hure [a], Marcela Trapé [a], Claudia Trossero [a], Gabriel Molina [a], Claudia Drogo [a], Patricia A.M. Williams [b], Ana María Atria [c], Juan Carlos Muñoz Acevedo [c], Susana Zacchino [d], Maximilano Sortino [d], Darío Campagnoli [e], Marcela Rizzotto [a,*]

[a] *Área Química Inorgánica, Suipacha 531, 2000 Rosario, Argentina*
[b] *CEQUINOR, Facultad de Ciencias Exactas, UNLP, cc. 962, La Plata, Argentina*
[c] *Facultad de Ciencias Químicas y Farmacéuticas, Universidad de Chile, Casilla 233, Santiago, Chile*
[d] *Área Farmacognosia, Universidad Nacional de Rosario, Suipacha 531, 2000 Rosario, Argentina*
[e] *Facultad de Ingeniería Química, UNL, Santiago del Estero, 2829-3000 Santa Fe, Argentina*

Abstract

The reaction between sulfathiazole and cobalt(II) leads to a pink solid, $[Co^{II}(ST)_2(H_2O)_4]$ (**1**), which, after 7–10 days in the mother solution, transforms into red crystals of $[Co^{II}(ST)_2(H_2O)_3]_n$ (**2**) (ST = sulfathiazolate). The Co(II) ion exhibits an octahedral environment in both compounds. Differences between them were noted in the IR spectra in the region corresponding to signals of the amine group. Antifungal properties of (**1**) were evaluated, showing activity against both *Aspergillus fumigatus* (the same as the ligand) and *Aspergillus flavus* (better than the ligand).

Keywords: Sulfathiazole; Sulfadrugs metal complexes; Cobalt complexes; Antifungal properties

1. Introduction

Among the many and so different families of organic–inorganic chemicals being currently investigated because of their applications, sulfonamides and their N-derivatives are one of the outstanding groups [1].

Sulfonamides were the first effective chemotherapeutic agents employed systematically for the prevention and cure of bacterial infections in humans [2,3]. After the introduction of penicillin and other antibiotics, the popularity of sulfonamides decreased. However, they are still considered useful in certain therapeutic fields, especially in the case of ophthalmic infections as well as infections in the urinary and gastrointestinal tract [4]. Besides, sulfadrugs are still today among the drugs of first election (together with ampicillin and gentamycin) as chemotherapeutic agents in bacterial infections by *Escherichia coli* in humans [5]. The sulfanilamides exert their antibacterial action by the competitive inhibition of the enzyme dihydropterase synthetase towards the substrate *p*-aminobenzoate [6]. Sulfathiazole, (4-amino-*N*-2-thiazolylbencenosulfonamide), HST (Fig. 1), is clinically one of the most used [7].

Neutral sulfonamides are expected to be poor ligands because of the withdrawal of the electron density from

* Corresponding author. Tel.: +543414219910; fax: +543414350214.
E-mail addresses: mrizzott@fbioyf.unr.edu.ar, mrizzot@agatha.unr.edu.ar (M. Rizzotto).

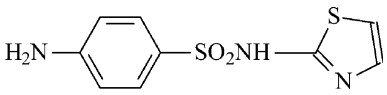

Fig. 1. Sulfathiazole (HST).

the nitrogen atom onto the electronegative oxygen atoms. However, if the sulfonamide N atom bears a dissociable hydrogen atom, this same electron-withdrawing effect increases its acidity and, in the deprotonated form, sulfonamide anions are effective σ-donor ligands [8]. On the other hand, complex formation between metal ions and sulfadrugs, pointing to the combined antibacterial activity of sulfonamides and the antimicrobial activity of heavy metals in some cases, and the activity of the metal complexes themselves, constitute an important field of research [1,2]. Furthermore, sulfadrugs and their metal complexes possess many applications, in addition to antibacterial activity such as diuretic, antiglaucoma or antiepileptic drugs, among others [9–14], like antifungal activity [15,16], and, in many cases, the activity of the metal complex is much better than the ligand alone [1].

Although the synthesis of metal complexes of sulfathiazole has been reported, the structural determination is often incomplete and conflicting [17,18]. Relating to sulfathiazole metal complexes, different compounds were reported in which the sulfathiazole moiety acts with a high versatility in its coordination ability. For example, with Zn(II) the drug acts as a bridging ligand through both the N_{amino} and $N_{thiazole}$ atoms [18]. As a neutral ligand, HST acts as a monodentate ligand, binding the metal ion through the N_{amino} atom [19]. As a deprotonated ligand, ST^- has a variety of coordination behaviors, e.g., besides the Zn(II)–ST complex [18], in Cu(II) complexes coordination through the N-thiazole atom could be seen, and in another case the sulfathiazolato exhibits bidentate behavior linking the metal ion through the $N_{thiazolic}$ and the $N_{sulfonamido}$ atoms [20]. More recently, we have analyzed the interaction of mercury(II) with sulfathiazole: IR and NMR spectral studies suggested a coordination of Hg(II) with the $N_{thiazolic}$ atom, unlike the related Hg-sulfadrugs compounds [21].

Despite its low availability in the earth's crust [22], cobalt plays important roles in biological systems. The most common examples are vitamin B_{12} and coenzyme B_{12}, a cofactor required for a group of enzymatic systems of central importance in biochemistry [23]. Cobalt is vitamin B_{12}'s only apparent biological site. Vitamin B_{12}-deficiency causes the severe disease of pernicious anemia in humans, which indicates the critical role of cobalt. The cobalt in vitamin B_{12} is coordinated to five N atoms, four attributed to a tetrapyrrole (corrin); the sixth ligand is C, provided either by C5 of deoxyadenosine in enzymes such as methylmalonyl-CoA (fatty acid metabolism) or by a methyl group in the enzyme that synthesizes the amino acid methionine in bacteria [24]. Besides, cobalt in organometallic complexes, has been shown to display a wide-ranging reactivity which includes alkyl transfer reactions and insertion reactions of small molecules such as O_2 and SO_2 into metal–alkyl bonds [25]. Because of its high sensitivity to the coordination site geometry and the many experimental techniques that can be used in its characterization, cobalt has been used to replace other metal ions to gather information about changes in metal sites in proteins during protein function [26–29]. Spectroscopic characterization of these systems has revealed that cobalt can be present as Co(II) and Co(III) ions in several types of coordination, which lead to different electronic and magnetic properties. In this context, the use of simple Co-containing systems with low molecular weight ligands is useful for understanding the correlation between spectroscopic and structural properties.

As part of a research program dedicated to the investigation of the structural, physicochemical and biological properties of metal complexes of sulfadrugs, the present paper reports the synthesis, spectral, structure and antifungal studies of compounds of sulfathiazole with Co(II), Co(II)–ST.

2. Experimental

2.1. Materials and methods

Sulfathiazole, as a sodium salt (Sigma, >99%), cobalt (II) chloride hexahydrate (Merck, GR), and all other chemicals of commercially available reagent grade were used as received.

The content of Co was determined by both complexometric back-titration with EDTA (ethylenediaminetetraacetic acid) [30,31] and atomic absorption spectroscopy with a double beam Perkin–Elmer spectrometer, model 3110, at UNL.

Elemental chemical analyses (C, H, N, S) were performed in a microanalyser Carlo Erba EA1108.

IR spectra of powdered samples were measured with a Bruker IFS 66 FTIR-spectrophotometer from 4000 to 400 cm^{-1}, using the KBr pellet technique. The Raman spectrum was measured with a Spex-Ramalog double monochromator spectrometer, using the 514.5 nm line of an Ar ion laser for excitation, over the region 200–2000 cm^{-1}.

Thermogravimetric (TG) and differential thermal analysis (DTA) were performed on a Shimadzu system (models TG-50 and DTA-50, respectively), working in an oxygen flow (50 mL/min) and a heating rate of 10 °C/min. Sample quantities ranged between 10 and 20 mg. Al_2O_3 was used as a DTA standard.

Room temperature magnetic susceptibility was determined with a Cahn-2000 balance, calibrated with $Hg[Co(SCN)_4]$ and at a magnetic field strength of 6 kG.

Electronic spectra were recorded between 200 and 800 nm in a Jasco model 530 double beam spectrophotometer using quartz cells of 1 cm path length at room temperature and in the following solvents: water, methanol (both in order to observe ligand transitions) and DMSO (for d–d transitions). Diffuse reflectance spectra were recorded with a Shimadzu UV-300 instrument, using MgO as an internal standard.

EPR spectroscopy: X-band EPR spectra were recorded as the first derivative of absorption on a Bruker EMX spectrometer operating at 77 K. The microwave frequency was generated with a Bruker 04 ER (9–10 GHz) and measured with a Bruker EMX 048T frequency meter. The magnetic field was measured with a Bruker EMX 035M NMR-probe gaussmeter. Spectral parameters were: 100 kHz field modulation, 10.0 G modulation amplitude, ca. 9.31 GHz microwave frequency, 5.6×10^3 receiver gain, CF = 2000 G, sweep width: 3950 G. Measurements were done on ca. 0.1 mL volume samples of DMSO frozen solution of Co(II)–ST, both pink powder and red crystals, drawn into a plane cell. Typically 1024 points were accumulated per spectrum. Number of scans: 3

Despite Co^{2+} being an excellent paramagnetic shift ion in protein NMR studies [32], it was not possible to take NMR spectra of the complexes because of the paramagnetism observed.

2.2. X-ray crystal structure determination

Highly redundant diffractometer data sets were collected at room temperature ($T = 295$ K) for compound (**2**), up to a 2θ max. of ca. 58°, with a Bruker AXS SMART APEX CCD diffractometer using monochromatic Mo Kα radiation, $\lambda = 0.71069$ Å, and a 0.3° separation between frames. Data integration was performed using SAINT and a semi-empirical absorption correction was applied using SADABS, both programs being included in the diffractometer package. The structure resolution was achieved by Patterson methods and difference Fourier. The structure was refined by least squares on F^2, with anisotropic displacement parameters for non-H atoms. Hydrogen atoms attached to carbon (C–H's) were placed at their calculated positions and allowed to ride onto their host carbons both in coordinates as well as in thermal parameters. Terminal methyl groups were allowed to rotate as well. Hydrogen atoms deemed as potentially active in H-bonding interactions (O–H's and N–H's) were searched in the late Fouriers, and treated in accordance to the data set qualities. In the structure, the amino H atoms [N(6)] were found in the final difference Fourier map and were refined to ensure a reasonable geometry.

All calculations to solve the structures, refine the proposed models and obtain derived results were carried out with the computer programs SHELXS97, SHELXL97 [33a] and SHELXTL/PC [33b]. Relevant parameters of the crystal structure determination are listed in Table 1.

2.3. Biological evaluation

Microorganisms and media: The microorganisms used for the fungistatic evaluation were purchased from the American Type Culture Collection (identified with the initials ATCC) Rockville, MD, USA, or were clinical isolates from CEREMIC, (identified with the capital letter C), Centro de Referencia Micológica, Facultad de Ciencias Bioquímicas y Farmacéuticas, Suipacha 531-(2000)-Rosario, Argentina. *Candida albicans* ATCC 10231, *Saccharomyces cerevisiae* ATCC 9763, *Cryptococcus neoformans* ATCC 32264, *Aspergillus flavus* ATCC 9170, *Aspergillus fumigatus* ATCC 26934, *Aspergillus niger* ATCC 9029, *Trichophyton mentagrophytes* ATCC 9972, *Trichophyton rubrum* C113, *Microsporum gypseum* C115 and *Candida tropicalis* C131 were grown on Sabouraud-chloramphenicol agar slants for 48 h at

Table 1
Crystal data and structure refinement for (**2**)

Identification code	(**2**)
Empirical formula	$C_{18}H_{22}CoN_6O_7S_4$
Formula weight	621.46
Temperature (K)	297(2)
Wavelength (Å)	0.71073
Crystal system	monoclinic
Space group	*Pn*
Unit cell dimensions	
a (Å)	10.2964(13)
b (Å)	10.2680(13)
c (Å)	12.0091(15)
α (°)	90
β (°)	103.067(2)
γ (°)	90
Volume (Å^3)	1236.8(3)
Z	2
Density (calculated) (Mg/m^3)	1.653
Absorption coefficient (mm^{-1})	1.083
F(000)	626
Crystal size (mm)	0.20 × 0.10 × 0.08
Theta range for data collection (°)	1.98 to 27.98
Index ranges	$-12 \leqslant h \leqslant 13$, $-13 \leqslant k \leqslant 12$, $-15 \leqslant l \leqslant 15$
Reflections collected	10009
Independent reflections	5146 [$R_{int} = 0.0446$]
Completeness to theta = 26.00° (%)	99.7
Absorption correction	Φ scans
Maximum and minimum transmission	1.0 and 0.792409
Refinement method	full-matrix least-squares on F^2
Data/restraints/parameters	5146/2/333
Goodness-of-fit on F^2	0.990
Final *R* indices [$I > 2\sigma(I)$]	$R_1 = 0.0563$, $wR_2 = 0.1132$
R indices (all data)	$R_1 = 0.0794$, $wR_2 = 0.1232$
Absolute structure parameter	0.01(2)
Largest difference peak and hole (e/Å^3)	0.472 and −0.304

30 °C. Cell suspensions in sterile distilled water were adjusted to give a final concentration of 10^6 viable yeast cells/mL [34].

The strains were maintained on slopes of Sabouraud-dextrose agar (SDA, Oxoid) and subcultured every 15 days to prevent pleomorphic transformations. Spore suspensions were obtained according to reported procedures [34] and adjusted to 10^6 spores with colony forming ability/mL.

2.4. Antifungal assays

The antifungal activity was evaluated with the agar dilution method by using Sabouraud-chloramphenicol agar for both yeast and dermatophyte species as previously described [35,36]. Stock solutions of compounds (10 mg/mL in DMSO) were diluted to give serial twofold dilutions that were added to each medium resulting in concentrations ranging from 0.10 to 250 mg/mL. MIC for each compound was defined as the lowest concentration that produces no visible fungal growth after the incubation time. Amphotericin B (Janssen Pharmaceutica, Belgium), Ketoconazole (Sigma Chemical Co., St. Louis, MO, USA) and Terbinafine (Novartis, Bs. As., Argentina) were used as positive controls.

2.5. Preparation of the complexes

2.5.1. $[Co(II)(ST)_2(H_2O)_4]$ (1)

10 mL of an aqueous solution of cobalt chloride containing 0.2377 g (1 mmol) of $CoCl_2 \cdot 6H_2O$, was added dropwise to 20 mL aqueous solution of sulfathiazole as the sodium salt, NaST, containing 0.6101 g NaST (2.2 mmol), with stirring at room temperature [2,21]. Immediately, the resulting mixture became blue, because a blue precipitate was formed. Then, the reaction mixture was left to stand at room temperature, away from light. After 4 days the precipitate, which turned into a pink solid, was centrifuged, washed with water several times, filtered off and dried under vacuum, away from light. Yield: 0.567 g, 88.6%.

2.5.2. $[Co(II)(ST)_2(H_2O)_3]_n$ (2)

After several attempts, when the concentrations of both reactive solutions for the obtainment of (**1**) were twice that reported above, the pink precipitate, left in the mother solution between 7 and 10 days, changed into little single red crystals (**2**), suitable for X-ray structural analysis. After 10–12 days, the red crystals were centrifuged, washed with water several times, filtered off and dried under vacuum, away from light. Yield: 0.547 g, 88.0%. Elemental analyses of the red crystals gave satisfactory results for $Co(II)(ST)_2(H_2O)_3$. Found (calc. for $CoC_{18}H_{22}N_6S_4O_7$): C, 34.1 (34.8); H, 3.0 (3.6); N, 13.3 (13.5); S, 21.2 (20.6); Co: 10.2 (9.5). It was not possible to obtain (**2**) from suspensions of (**1**) in water, in the presence and absence of: NaST and NaST plus Co(II), in several concentrations, left about 20 days at room temperature.

3. Results and discussion

3.1. General physicochemical characteristics of (1)

Elemental analyses of the pink powder gave satisfactory results for $Co(II)(ST)_2(H_2O)_4$. Found (calc. for $CoC_{18}H_{24}N_6S_4O_8$): C, 34.2 (33.8); H, 3.2 (3.8); N, 13.0 (13.1); S, 19.8 (20.1); Co: 9.9 (9.2). Compound (**1**) is only slightly soluble in water at room temperature (38 mg/100 mL), but it is soluble in DMSO. In a HCl 1 M solution it suffers hydrolysis, and turns brownish in NaOH 1 M solution, maybe due to oxidation by means of the atmospheric oxygen.

3.2. Crystal description of (2)

The structure of the complex (**2**), $[Co^{II}(ST)_2(H_2O)_3]_n$ as determined by means of X-ray diffraction, resulted in a polymeric chain along the 1 0 1 direction. The repeating unit of this chain is a monomeric entity built up of one cobalt atom bonded to three nitrogen atoms from three different ST ligands, N1 of a hanging ST monodentate ligand, N(4) of a bridging ST group and N(6) coming from a neighboring monomeric unit. Completing the coordination sphere three oxygen atoms from water molecules were found (Fig. 2). The cobalt atom exhibits a distorted octahedral coordination sphere. The basal plane of this octahedral sphere is formed by Co(1) N(1) N(4) O(6) N(6A) (with a minimum plane deviation of 0.0174 Å); O(5) and O(7) occupy the apical positions. The Co–O bond distances vary between 2.109 and 2.195 Å and the Co–N distances vary

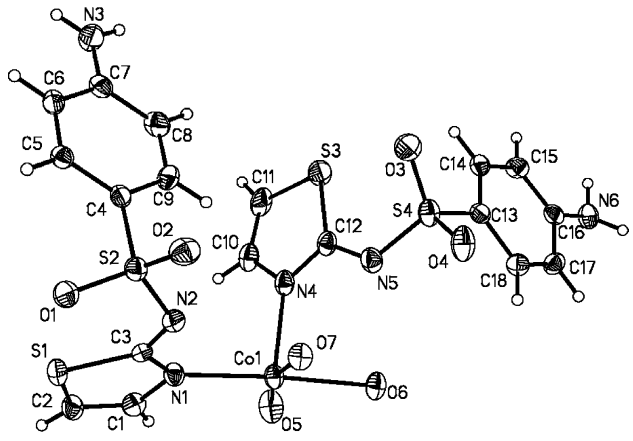

Fig. 2. Structure and atom numbering scheme for (**2**). XP view (Sheldrick, 1994), thermal ellipsoids at 50% probability level.

from 2.114 to 2.220 Å. A selected list of interatomic bond distances and angles are given in Table 2. The bond distances Co–O_{water} and Co–N found are similar to that in other cobalt(II) complexes, e.g., the Co–O_{water} bond distance is 2.090 Å in the complex [Co(L-threonine)$_2$(H_2O)$_2$] [37]. Co–N bond distances vary from 2.039 Å (Co–N_{NCS}) to 2.1951 Å (Co–N_{amino}) in the complex [Co(sulfacetamide)$_2$(NCS)$_2$] [1]. For the complex of cobalt(II) with sulfamethizolate, smtz, and pyridine, py, [Co(smtz)$_2$(py)$_2$(H_2O)], the Co–O_{water} bond distance is shorter (2.0457 Å) than in (**2**) and shorter than the Co–N distances (both $N_{thiadiazole}$ and N_{py}) in the same complex, because its geometry is a distorted octahedral one, with two sulfamethiazolate ligands in the equatorial sites and two water O atoms in the apical positions [38]. In the polymer {[Zn(smtz)$_2$(py)·H_2O]}$_\infty$, the Zn–$N_{thiadiazole}$ bond distances (1.962 and 1.989 Å) are slightly shorter than the Zn–N_{amino} ones (2.070 Å) [39], which is similar to that found in the complex Co(II)–ST (**2**). This fact seems to suggest that the thiazole N atom is able to bind the Co(II) ions much closer compared to the amino N atom, which can be due to the increase of the negative charge on the thiazole ring N atom as a consequence of the charge delocalization through the thiazole ring upon the deprotonation of the sulfonamido group [39].

The chains interact with each other by means of hydrogen bonding, involving the hydrogen atoms of the amino group of the hanging ST monodentate ligand and oxygen atoms of the sulfonamide group belonging to bridging ST group from a nearby chain [H3A···O3 = 2.512 Å, H3A···O4 = 2.680 Å] and also with an oxygen atom from a hanging ST monodentate ligand of the same nearby chain [H3B···O2 = 2.151 Å]. This hydrogen bonding scheme repeats throughout the complete crystal structure (Fig. 3).

Table 2
Selected bond lengths (Å) and angles (°) for (**2**)

Bond lengths (Å)		Angles (°)	
Co(1)–O(7)	2.109(4)	O(7)–Co(1)–N(4)	92.35(18)
Co(1)–N(4)	2.114(5)	O(7)–Co(1)–N(1)	96.47(17)
Co(1)–N(1)	2.128(5)	N(4)–Co(1)–N(1)	96.83(18)
Co(1)–O(5)	2.150(4)	O(7)–Co(1)–O(5)	165.55(17)
Co(1)–O(6)	2.195(4)	N(4)–Co(1)–O(5)	93.0(2)
Co(1)–N(6)#1	2.220(6)	N(1)–Co(1)–O(5)	96.20(18)
C(1)–C(2)	1.334(8)	O(7)–Co(1)–O(6)	80.92(16)
C(16)–N(6)	1.429(8)	N(4)–Co(1)–O(6)	87.88(17)
N(5)–S(4)	1.596(5)	N(1)–Co(1)–O(6)	174.74(18)
N(6)–Co(1)#2	2.220(6)	O(5)–Co(1)–O(6)	85.88(17)
O(1)–S(2)	1.460(4)	O(7)–Co(1)–N(6)#1	85.9(2)
O(2)–S(2)	1.436(5)	N(4)–Co(1)–N(6)#1	171.7(2)
O(3)–S(4)	1.436(4)	N(1)–Co(1)–N(6)#1	91.4(2)
O(4)–S(4)	1.432(4)	O(5)–Co(1)–N(6)#1	86.8(2)
		O(6)–Co(1)–N(6)#1	83.85(19)

Symmetry transformations used to generate equivalent atoms: #1: $x + 1/2, -y + 1, z - 1/2$; #2: $x - 1/2, -y + 1, z + 1/2$.

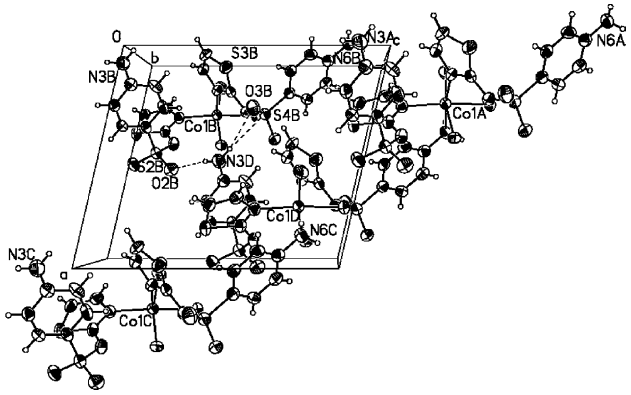

Fig. 3. Crystal packing of (**2**), showing a simplified hydrogen bonding scheme. XP view along *b* axes (Sheldrick, 1994), thermal ellipsoids at 50% probability level.

3.3. Infrared spectra

IR selected spectral data of the Co(II)–ST complexes (pink powder and red crystals) and the ligand (as sulfathiazole and its sodium salt) are presented in Table 3.

In the 3600–3000 cm^{-1} region, broad bands appear for NaST and Co(II)–ST (both pink powder and red crystals) due to the presence of hydration water [40,41]. The strong band at 1536 cm^{-1}, attributed in the sulfadrug to the thiazole ring vibration, was shifted to lower frequencies. This fact is in agreement with the interaction through the $N_{thiazole}$ atom [42]. In the two cobalt compounds the bands attributed to the SO_2 vibrations remain unaltered, suggesting no interaction of the –SO_2-group with the metal ion. This was confirmed for (**1**) by Raman spectroscopy: the symmetric stretching located at 1123 cm^{-1} increased its intensity as expected. According to the observed changes in the IR spectra of (**1**) and (**2**) it is possible to infer that the thiazole nitrogen atoms might be sites of coordination of the cobalt atom with the sulfathiazolato anions in

Table 3
Assignment of the vibrational spectra (frequency: υ, cm^{-1}) of sulfathiazole (HST), its sodium salt (NaST) and its Co(II) complex (Co(II)–ST), as pink powder (**1**) and red crystals (**2**)

HST	NaST	Co(II)–ST (**1**)	Co(II)–ST (**2**)	Assignments
	3589 m	3582 sh	masked	νOH
3346 m	3492 s	3460 s, br	3468 m	$\nu_{as}NH_2$
	3418 s		3443 m	
3320 m	3336 s	3358 s, br	3386 sh	ν_sNH_2
			3358 s	
	1622, m	1629 m	1629 m	δH_2O
1536 vs	1445 vs	1450 s	1445 s	thiazole ring
1324 m	1321 m	1316 m	1318 m	$\nu_{as}SO_2$
1138 s	1131 s	1123 vs	1146 m	ν_sSO_2
920 s	958 s	968 m	962 m	νSN
732 m				ωNH
573 s	569 m	577 m	572 m	ωSO_2
554 m	551 s	553 s	557 m	ωSO_2

both complexes. This conclusion is consistent with related systems containing sulfathiazole and different metal ions [21,43–46]. The differences that are noted in the region between 4000 and 3000 cm^{-1} of the IR spectra of (**1**) and (**2**) are probably due to differences in the coordination of the amino group in both complexes.

3.4. Thermogravimetric behavior

The thermal behavior of compounds HST and Co(II)–ST (**1**), pink powder, are shown in Fig. 4. The thermal degradation of sulfathiazole proceeds in four different stages. The first decomposition process takes place between 10 and 296 °C with about 18.4% weight loss (DTA signals: 175 °C (endo, w) and 207 °C (endo, w)). Upon further heating, the sample loses mass in two steps ($\Delta\omega$ = 8.6% and 6.1%) up to 425 °C, then the decomposition speeds up suddenly with a strong DTA signal at 514 °C (exo, s), giving volatile products.

In the case of Co(II)–ST (**1**), the sample first loses weight corresponding to four water molecules (observed 11.2%, calculated 11.3%) between 15 and 210 °C, DTA: 125 °C (endo, vw). On further heating the decomposition occurs in the range 210–1000 °C, showing that there are at least four chemical processes in progress, associated with three exothermic signals at 287 °C (exo, vw), 466 °C (exo, vw) and 576 °C (exo, vs). The final product, Co_2O_3, could be identified based on its IR spectrum. The final formation of Co_2O_3 entails $\Delta\omega$ = 87% in agreement with the experimental determination. Therefore, the following general decomposition scheme can be formulated:

$$[Co(ST)_2(H_2O)_4] \xrightarrow{\phi,O_2} Co_2O_3 + \text{other volatile products}$$

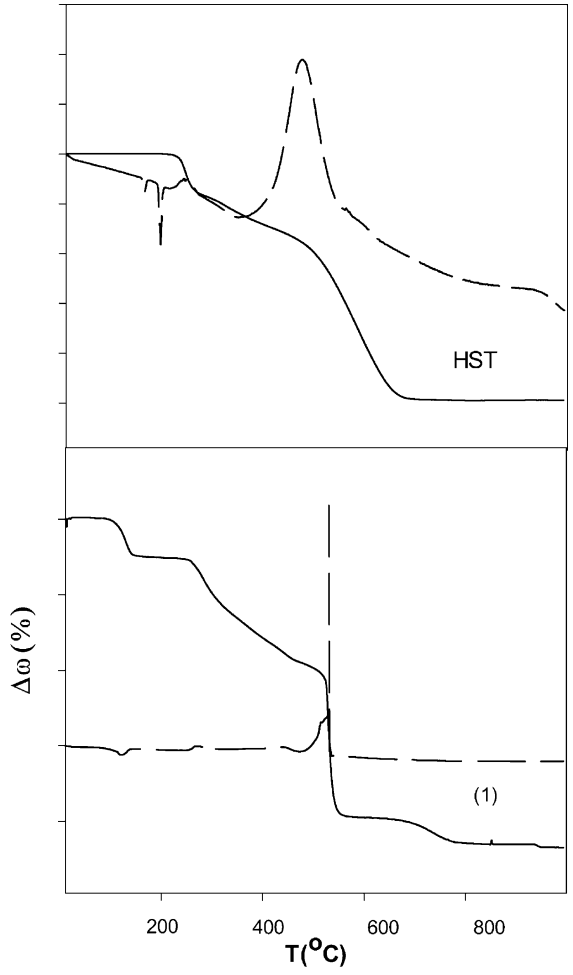

Fig. 4. TG (—) and DTA (- - -) traces for the thermal decomposition of HST and (**1**) system (O_2 flow = 60 cm^3/min, heating rate: 10 °C/min).

3.5. Magnetic behavior

The measured μ_{eff} for Co(II)–ST (1), 4.63 BM, is in the range of 4.1–5.2 BM according to the values expected for a d^7 (s = 3/2) system with spin–orbit coupling [47].

3.6. Electronic spectra

Electronic spectra of complexes can provide valuable information related to bond and structure, since the colors are intimately related to the magnitude of the spacing between d-orbitals (e_g and t_{2g} or e and t_2 orbitals in octahedral and tetrahedral complexes, respectively), which depends on factors such as the geometry of the complex, the nature of the ligands present and the oxidation state of the central metal atom [47].

The diffuse reflectance spectrum was measured in the 400–900 nm range. The spectrum of Co(II)–ST (**1**) suggests an octahedral geometry around the metal ion [48]. There can be observed two of the three possible electronic transitions: $\nu_2[^4T_{1g} \rightarrow {}^4A_{2g}]$ = 610 nm and $\nu_3[^4T_{1g} \rightarrow {}^4T_{1g}(P)]$, multiple structured at 532, 480 (sh) and 435 (sh) nm. The $\nu_1[^4T_{1g} \rightarrow {}^4T_{2g}]$ transition is expected at 1300 nm, outside the measured range.

3.6.1. Electronic spectra in solution

The wavelength of the absortion maxima, in nm, and their respective molar absortivity (ε, in $M^{-1}\,cm^{-1}$) are summarized for both (**1**) and $CoCl_2 \cdot 6H_2O$ in methanol and DMSO solutions in Table 4.

The electronic spectrum produced by $CoCl_2 \cdot 6H_2O$ in methanol seems very similar to that arising from the octahedral $[Co(H_2O)_6]^{2+}$ complex in water [49]. The major differences between the spectra of (**1**) and $CoCl_2 \cdot 6H_2O$ are observed in an aprotic solvent, DMSO, where the two bands observed ($\lambda 1$ and $\lambda 2$) are shifted to lower wavelength for (**1**). The absortion maxima for cobalt chloride in DMSO occur at 615 and 679 nm. The absortion maxima of (**1**) are shifted to lower wavelength respect to the maxima corresponding to $CoCl_2 \cdot 6H_2O$,

Table 4
Electronic spectra in solution

Compound	Solvent							
	Methanol				DMSO			
	$\lambda 1$	$\varepsilon 1$	$\lambda 2$	$\varepsilon 2$	$\lambda 1$	$\varepsilon 1$	$\lambda 2$	$\varepsilon 2$
$[Co(II)(ST)_2(H_2O)_4]$ (**1**)	531	33	620 (sh)		539	158	584	213
$CoCl_2 \cdot 6H_2O$	528	8	668	3	615	127	679	185

suggesting an increase in the ligand field strength [50]. Because their ε value in a protic solvent, the two spectra suggest an octahedral environment around the Co(II) ion, while for (**1**) in DMSO there is a tetrahedral arrangement around the Co(II) ion. Comparing both the color of the DMSO solution of (**1**) and the precipitate obtained in the first moment (which turn in a spontaneous way into the pink solid (**1**)), it is possible to suggest that the blue unstable solid obtained as the initial precipitate, could have a tetrahedral geometry around the Co(II) ion.

3.7. EPR measurements

X-band EPR spectra of a frozen DMSO solution of (**1**) and (**2**) were recorded at 77 K. Both spectra were very similar. The isotropic g value is close to 2.9. The hyperfine structure expected for the 100% abundant ^{59}Co isotope ($^{59}I = 7/2$) is not observed in the spectra of both samples (pink solid (**1**) and red crystals (**2**)). This suggests that the magnitude of the exchange interaction between Co(II) ions is larger than the magnitude of the hyperfine coupling parameter A, so the hyperfine structure collapses and gives a single collapsed peak [37]. The collapse of the hyperfine structure produces the observed Lorentzian line shape. A similar line shape EPR spectrum was observed for a complex of Co(II) and citric acid, at pH $\cong$ 5, in the form of its K^+ salt, at 4 K, which would produce mononuclear octahedral Co(II)–citrate species [51]. In the EPR spectrum of Co(II)–ST it is possible to observe a shoulder of the main resonance at a g value of ca. 3.4, which is absent in the Co(II)–citrate one. It might be probably due to the presence of N-atoms coordinated to cobalt in Co(II)–ST, in addition to O-atoms, while in Co(II)–citrate, there are only O-atoms coordinated to Co(II). Another difference with respect to the citrate system is that the resonance of Co(II)–ST is observable at 77 K, which suggests minor intensity of relaxation effects in the sulfathiazole system.

3.8. Antifungal activity

Some metal complexes of sulfadrugs promote rapid healing of skin disorders (e.g., the Ag(I)- and the Zn(II)-sulfadiazine) in preventing bacterial infection in burnt animals [52]. In addition to its well-known antibacterial activity, silver sulfadiazine was recently reported to possess strong antifungal properties [53], which makes it a clinically widely used topical agent for the treatment of wound and burnt infections [54].

Although several classes of antifungal compounds are presently available, resistance to these drugs constantly emerges [55] and it is of crucial importance to investigate new types of antifungal agents in order to prevent this serious medical problem. Metal ions (such as Zn(II)) or metal complexes with putative clinical applications were extensively studied in recent years [56]. Complexes of silver and zinc sulfonamides (and some cerium derivatives) have successfully been used for the last 20 years for the prophylaxis and treatment of microbial and fungal burnt wound infections and they seem to constitute a valuable alternative for resolving the resistance problem [57,58]. Results of the antifungal assay with (**1**) (and NaST in order to compare with the ligand) are showed in Table 5. Only the two species of the *Aspergillus* genus tested were susceptible to both compounds.

When tested against *A. fumigatus*, both compounds, Co(II)–ST (**1**) and NaST, showed the same MIC values suggesting that the activity could be due to the sulfathiazole moiety. In contrast, it is interesting to note that compound (**1**) inhibits *A. flavus* while the ligand NaST does not. This difference in activity could be due to the presence of the metal in the complex which, according with previous reports, might exert its antifungal action by inhibition of enzymes that are involved in the biosynthesis of cell walls of fungi [59].

Table 5
MIC values (μg/mL)[a] of sodium sulfathiazole (NaST) and the Co(II)–sulfathiazolate complex $[Co^{II}(ST)_2(H_2O)_4]$ (**1**) acting against human opportunistic pathogenic fungi

	NaST	(**1**)	Amp	Ket	Terb
C. albicans	>250	>250	0.75	0.50	
C. tropicalis	>250	>250	0.50	0.125	
S. cerevisiae	>250	>250	0.50	0.50	
C. neoformans	>250	>250	0.40	0.25	
A. fumigatus	200	200	3.00	12.50	
A. flavus	>250	100	3.00	2.00	
A. niger	>250	>250	0.90	12.50	
M. gypseum	>250	>250	0.12	0.05	0.01
T. rubrum	>250	>250	0.75	0.25	0.04
T. mentagrophytes	>250	>250	0.10	0.05	0.01

[a] The MIC was confirmed by two replicates. Amp: Amphotericin B; Ket: Ketoconazole; Terb, Terbinafine *Candida albicans* ATCC 10231; *C. tropicalis C Cryptiococccus neofiormans* ATCC 32264; *Saccharomyces cerevisiae* ATCC 9763; *Aspergillus fumigatus* ATCC 26934; *A. flavus* ATCC 9170; *A. niger* ATCC 9029; *Microsporum gypseum* C 115, *Trichophyton rubrum* C 113, *Trichophyton mentagrophytes* ATCC 9972. ATCC: American Type Culture Collection (Rockville, MD, USA); C: CEREMIC, Centro de Referencia Micológica, Facultad de Ciencias Bioquímicas y Farmacéuticas, Suipacha 531-(2000)-Rosario, Argentina.

4. Conclusion

The reaction between sulfathiazole and cobalt(II) leads to two stable compounds, obtained in sequencial steps, whose molecular formulas differ from each other by one water molecule. The IR spectra of both compounds differ in the region of the signals of the amino group. The 6th position around Co(II), which in (**2**) is filled with the amino group of a sulfathiazolate moiety – acting as a bidentated ligand – would be filled with a water molecule in (**1**).

The metal complex Co(II)–ST (**1**) displayed a moderate antifungal activity against both species of *Aspergillus* tested. This activity was showed to be the same as that of the corresponding ligand NaST against *A. fumigatus* but interestingly, it marked an important difference with the antifungal behavior of NaST against *A. flavus*, which was not inhibited by the ligand up to 250 μg/mL.

5. Supporting information available

CCDC 239368 contains the supplementary crystallographic data for this paper. These data can be obtained free of charge via www.ccdc.cam.ac.uk/data_request/cif, by emailing data_request@ccdc.cam.ac.uk, or by contacting the Cambridge Crystallographic Data Centre, 12, Union Road, Cambridge CB2 1EZ, UK; fax: +44 1223 336033.

Acknowledgements

We are grateful for funding from FONDECYT 1020122. J.C.M.A. is a grateful recipient of a Deutscher Akademischer Austauschdienst scholarship. P.A.M.W. is member of the Carrera del Investigador CICPBA. M.R. is member of the Carrera del Investigador CIC-UNR. We also thank Dr. Aviva Levina for the registration of the EPR spectra. S.Z. gives thanks to Agencia de Promociones Científicas y Tecnológicas de Argentina, ANPCyT (PICTR 260) and to Project X.7-PIBEAFUN (Iberian–American Project on Search and Development of Antifungal Agents) of the Iberian-American Program for the Development of Science and Technology (CYTED).

References

[1] F. Blasco, L. Perelló, J. Latorre, J. Borrás, S. Garciá-Granda, J. Inorg. Biochem. 61 (1996) 143.
[2] A. Bult, in: H. Sigel (Ed.), Metal Ions in Biological Systems, 16, Marcel Decker, New York, 1983, p. 261.
[3] Th. Nogrady, Medicinal Chemistry, 2nd ed., Oxford University Press, New York, 1988, p. 383.
[4] E.R. Barnhart (Ed.), Physician's Desk Reference, PDR, 43rd ed., Medical Economics, New York, 1989.
[5] G. Mandell, M. Sande, in: A. Goodman, L. Gilman (Eds.), Las Bases Farmacológicas de la Terapéutica, 6th ed., Ed. Médica Panamericana, Buenos Aires, 1981.
[6] A. García-Raso, J.J. Fiol, S. Rigo, A. López-López, E. Molins, E. Espinosa, E. Borrás, G. Alzuet, J. Borrás, A. Castiñeiras, Polyhedron 19 (2000) 991.
[7] J. Casanova, G. Alzuet, J. Borrás, L. David, D. Gatteschi, Inorg. Chim. Acta 211 (1993) 183.
[8] G. Alzuet, S. Ferrer-Llusar, J. Borrás, J. Server-Carrió, R. Martínez-Máñez, J. Inorg. Biochem. 75 (1999) 189.
[9] A. Bonamartini Corradi, E. Gozzoli, L. Menabue, M. Saladini, L.P. Battaglia, P. Sgarabotto, J. Chem. Soc., Dalton Trans. (1994) 273.
[10] S. Ferrer, J. Borrás, E. Garcia-España, J. Inorg. Biochem. 39 (1990) 297.
[11] C.T. Supuran, F. Mincione, A. Scozzafava, F. Briganti, G. Mincinone, M.A. Ilies, Eur. J. Med. Chem. 33 (1998) 247.
[12] C.T. Supuran, A.J. Scozzafava, Enzyme Inhib. 13 (1997) 37.
[13] A. Jitianu, M.A. Ilies, A. Scozzafava, C.T. Supuran, Main Group Met. Chem. 20 (1997) 14.
[14] A. Scozzafava, L. Menabuoni, F. Mincione, F. Briganti, G. Mincinone, C.T. Supuran, J. Med. Chem. 42 (1999) 2641.
[15] M. Barboiu, M. Cimpoesu, C. Guran, C.T. Supuran, Metal Base Drugs 3 (1996) 227.
[16] F. Briganti, A. Scozzafava, C.T. Supuran, Eur. J. Med. Chem. 32 (1997) 901.
[17] M.H. Torre, G. Facchin, E. Kremer, E. Castellano, O.E. Piro, E.J. Baran, J. Inorg. Biochem. 94 (2003) 200.
[18] J. Casanova, G. Alzuet, S. Ferrer, J. Borrás, S. García-Granda, E. Perez-Carreño, J. Inorg. Biochem. 51 (1993) 689.
[19] J. Casanova, G. Alzuet, J. Borrás, J. Timoneda, S. García-Granda, I. Cándano-García, J. Inorg. Biochem. 56 (1994) 65.
[20] J. Casanova, G. Alzuet, J. Latorre, J. Borrás, Inorg. Chem. 36 (1997) 2052.
[21] S. Bellú, E. Hure, M. Trapé, M. Rizzotto, E. Sutich, M. Sigrist, V. Moreno, Quím. Nova 26 (2003) 188.
[22] S.J. Lippard, J.M. Berg, Principles of Bioinorganic Chemistry, University Science Books, Mill Valley, CA, 1994.
[23] J.J.R. Fraústo da Silva, R.J.P. Williams, The Biological Chemistry of the Elements, Clarendon Press, Oxford, 1997.
[24] I. Bertini, H. Gray, S. Lippard, J. Valentine, Bioinorganic Chemistry, University Science Books, Mill Valley, CA, 1994.
[25] R. Dreos, A. Felluga, G. Nardin, L. Randaccio, P. Siega, G. Tauzher, Inorg. Chem. 40 (2001) 5541.
[26] E. Carvalho, R. Aasa, P. Göthe, J. Inorg. Biochem. 62 (1996) 147.
[27] N. Bonander, T. Vänngard, L. Tsai, V. Langer, H. Nar, L. Sjölin, Proteins 27 (1997) 385.
[28] A. Adrait, L. Jacquamet, L. Pape, A. González de Peredo, D. Aberdam, J.L. Hazemann, J.M. Latour, I. Michaud-Soret, Biochemistry 38 (1999) 6248.
[29] K.R. Strand, S. Karlsen, K.K. Andersson, J. Biol. Chem. 277 (2002) 34229.
[30] G. Schwarzenbach, H. Flaschka, Complexometric Titration, Methuen, London, 1969.
[31] I.M. Kolthoff, E.B. Sandell, E.J. Meehan, Bruckenstein, S. Análisis Químico Cuantitativo, 6th ed. Editorial Nigar S.R.L., Buenos Aires, 1979.
[32] J. Cowan, Inorganic Biochemistry an Introduction, VCH, New York, 1993.
[33] (a) G.M. Sheldrick, SHELXS-97 and SHELXL-97. Programs for structure resolution and refinement, University of Göttingen, Göttingen, Germany, 1997;
(b) G.M. Sheldrick, SHELXTL_PC Version 5.0, Siemens Analytical X-ray Instruments Inc., Madison, WI, USA, 1994.

[34] L.R. Wright, E.M. Scott, S.P. Gorman, J. Antimicrob. Chemother. 12 (1983) 317.
[35] S.A. Zacchino, G.E. Rodríguez, G. Pezzenati, G. Orellana, R.D. Enriz, M. Gonzalez Sierra, J. Nat. Prod. 60 (1997) 659.
[36] S.A. Zacchino, S.N. López, G. Pezzenati, R.L. Furlán, C.B. Santecchia, L. Muñoz, F.A. Giannini, A.M. Rodríguez, R.D. Enriz, J. Nat. Prod. 62 (1999) 1353.
[37] A. Rizzi, C. Brondino, R. Calvo, R. Baggio, M.T. Garland, R. Rapp, Inorg. Chem. 42 (2003) 4409, and references therein.
[38] E. Borrás, G. Alzuet, J. Borrás, J. Server-Carrió, A. Castiñeiras, M. Liu-González, V. Sanz-Ruiz, Polyhedron (2000) 1859.
[39] G. Alzuet, J. Borrás, F. Estevan, M. Liu-González, F. Sanz-Ruiz, Inorg. Chim. Acta 343 (2003) 56.
[40] D. Lin Vien, N.B. Colthup, W.F. Fateley, J.G. Grasselli, Infrared and Raman Characteristic Frequencies of Organic Molecules, Academic Press, Boston, MA, 1991.
[41] B. Smith, Infrared Spectral Interpretation. A Systematic Approach, CRC Press, New York, 1999.
[42] B. Simó, L. Perelló, R. Ortiz, A. Castiñeira, J. Latorre, E. Cantón, J. Inorg. Biochem. 81 (2000) 275.
[43] J. Casanova, G. Alzuet, S. Ferrer, J. Latorre, J.A. Ramírez, J. Borrás, Inorg. Chim. Acta 304 (2000) 170.
[44] M. González-Álvarez, G. Alzuet, J. Borrás, B. Macías, M. Del Olmo, M. Liu-González, F. Sanz, J. Inorg. Biochem. 89 (2002) 29.
[45] R. Yuan, R. Xiong, Z. Chen, P. Zhang, H. Ju, Z. Dai, Z. Guo, H. Fun, X. You, J. Chem. Soc., Dalton Trans. (2001) 774.
[46] E. Chufán, J. Pedregosa, J. Borrás, Vibr. Spectrosc. 15 (1997) 191.
[47] J. Huheey, E. Keiter, R. Keiter, Inorganic Chemistry: Principles of Structure and Reactivity, Harper Collins, New York, 1993.
[48] A.B.P. Lever, Inorganic Electronic Spectroscopy, 2nd ed., Elsevier, The Netherlands, 1984.
[49] F.A. Cotton, G. Wilkinson, Advanced Inorganic Chemistry, 4th ed., Wiley, New York, 1980.
[50] C. Comussi, M. Grespan, P. Polese, R. Portanova, M. Tolazzi, Inorg. Chim. Acta 321 (2001) 49.
[51] N. Kotsakis, C.P. Raptopoulou, A. Terzis, J. Giapintzakis, T. Jakusch, T. Kiss, A. Salifoglou, Inorg. Chem. 42 (2003) 22.
[52] A. García-Raso, J.J. Fiol, G. Martorell, A. López-Zafra, M. Quirós, Polyhedron 16 (1997) 613.
[53] J.B. Wright, K. Lam, D. Hansen, R.E. Burrell, Am. J. Infect. Control 27 (1999) 344.
[54] A.J. Singer, L. Berrutti, S.A. McClain, Wound Repair Regen. 7 (1999) 356.
[55] K. Asai, N. Tsuchimori, K. Okonogi, J.R. Perfect, O. Gotoh, Y. Yoshida, Antimicrob. Agents Chemother. 43 (1999) 1163.
[56] A.Y. Louie, T. Meade, J. Chem. Rev. 99 (1999) 2711.
[57] N. George, J. Faoagali, M. Muller, Burns 23 (1997) 493.
[58] P. Marone, V. Monzillo, L. Perversi, E. Carretto, J. Chemother. 10 (1998) 17.
[59] A. Mastrolorenzo, A. Scozzafava, C. Supuran, Eur. J. Pharm. Sci. 11 (2000) 99.